Coexistence of extended and localized states in the one-dimensional non-Hermitian Anderson model

Cem Yuce [1] and Hamidreza Ramezani [2]
[1]*Department of Physics, Eskisehir Technical University, Eskisehir 26000, Turkey*
[2]*Department of Physics and Astronomy, University of Texas Rio Grande Valley, Edinburg, Texas 78539, USA*

(Received 27 February 2022; revised 19 April 2022; accepted 5 July 2022; published 18 July 2022)

In one-dimensional Hermitian tight-binding models, mobility edges separating extended and localized states can appear in the presence of properly engineered quasiperiodical potentials and coupling constants. On the other hand, mobility edges do not exist in a one-dimensional Anderson lattice since localization occurs whenever a diagonal disorder through random numbers is introduced. Here we consider a nonreciprocal non-Hermitian lattice and show that the coexistence of extended and localized states appears with or without diagonal disorder in the topologically nontrivial region. We discuss that the mobility edges appear basically due to the boundary condition sensitivity of the nonreciprocal non-Hermitian lattice.

DOI: 10.1103/PhysRevB.106.024202

I. INTRODUCTION

Anderson localization (AL), a well-understood fundamental problem in condensed matter, is the absence of diffusion of waves in a disordered medium due to interference of waves [1]. Specifically in AL, all states are exponentially localized in the presence of any disorder in a one- and two-dimensional Anderson model at which a random disordered on-site potential is introduced. On the other hand, for weak disorder, if the localization length is bigger than the system size, then the system behaves as it is delocalized. In three dimensions we would have a mobility edge separating localized and extended states. Contrary to the one-dimensional (1D) Anderson model, in the Aubry-André model in which its disorder is modeled as a quasiperiodic on-site potential depending on the strength of incommensurate potential, all states are localized or delocalized [2]. This means that the system can undergo a metal-insulator transition even in 1D. However, this transition is sharp, i.e., all single-particle eigenstates in the spectrum suddenly become exponentially localized above a threshold level of disorder. In both cases, localized and extended states generally do not coexist since none of these models possess a mobility edge in 1D, i.e., critical energy separates localized and delocalized energy eigenstates. Recent studies show that the transition is not sharp beyond the one-dimensional Aubry-André model with correlated disorder and hopping amplitudes. It was shown that an intermediate regime characterized by the coexistence of localized and extended states at different energies may occur [3–8]. The theoretical findings were confirmed in an experimental realization of a system with a single-particle mobility edge [9]. There is a vast literature on mobility edges in Hermitian systems, but it has only been recently that mobility edges have been explored for various 1D tight-binding non-Hermitian models [10–29]. The first such model was considered in the pioneering paper by Hatano and Nelson [49]. In non-Hermitian systems, in comparison to the Hermitian ones, the mobility edges not only separate localized states from the extended states but also indicate the coexistence of complex and real energies. The latter allows us to come out with a topological characterization of mobility edges [11]. Apart from these models, extended and localized states can coexist in some other Hermitian lattices with an inhomogeneous trap [30,31] and with a partially disordered potential [32]. In general, such systems require complicated engineering of the hopping parameters and on-site potentials [33].

In this work we consider non-Hermitian extensions of the one-dimensional Anderson and Aubry-André-Harper models with asymmetric (nonreciprocal) hopping amplitudes at which a non-Hermitian skin effect (NHSE) plays important roles on the localization [34–48]. We introduce mixed boundary conditions (MBC) as a mixture of periodic (PBC) and open (OBC) boundary conditions and show that extended and localized states can coexist even for the lattice without the disorder. We show that extended states form a closed loop in the complex energy plane while the localized states have real energies. We further explore the effect of on-site potentials and show that localized and extended states survive in the presence of the on-site potentials until topological phase transition occurs at strong disorder and all states are localized.

II. MODEL

The starting point of our analysis is provided by the one-dimensional nonreciprocal lattice with asymmetric nearest-neighbor couplings and on-site potentials. The field amplitudes ψ_n at various sites of the lattice can be obtained by solving

$$J_R\,\psi_{n-1} + J_L\,\psi_{n+1} + V_n\,\psi_n = E\,\psi_n, \tag{1}$$

where $n = 1, 2, \ldots, N$ with N being the total number of sites, J_L and J_R are positive-valued coupling constants in the left and right directions, respectively, and V_n are real-valued on-site potentials. We assume $J_L > J_R$, unless otherwise stated. Two

different types of on-site potentials should be distinguished here. The first one is for the non-Hermitian Anderson model at which the on-site potentials are independent random potentials uniformly distributed in the interval $W[-\frac{1}{2}, \frac{1}{2}]$ with disorder strength W. This model exhibits an Anderson transition at a nonzero value of the disorder strength in contrast to the Hermitian system, whose eigenstates are always localized in the presence of a random potential [49,50]. The second one is for the non-Hermitian Aubry-André model at which the on-site potential is the quasiperiodic potential to describe an intermediate case between ordered and disordered systems, i.e., $V_n = V_0 \cos(2\pi\beta n)$, where V_0 is the amplitude of the on-site incommensurate potential and β is an irrational number. This model exhibits a metal-insulator transition when the potential strength is above a critical point [43].

The spectrum for the non-Hermitian lattice described by Eq. (1) shows strong sensitivity to the boundary conditions in the topologically nontrivial region [50]. Consider for example, the case without on-site potentials, which is topologically nontrivial as long as $J_L \neq J_R$. In this case, the spectrum describes a loop in the complex energy plane when the lattice has no edges (under PBC), whereas the spectrum is real when the lattice has two edges (under OBC). The change in the spectrum is also dramatic if the lattice has only one edge. In fact, there can be two such cases. The first one is the semi-infinite lattice ($N \to \infty$) whose spectrum fills the interior of the PBC loop in the complex plane. However, this case is not physical since any experiment naturally contains a finite number of lattice sites. The second one is the finite lattice with only one edge, i.e., the lattice has an open edge on the left and the other edge is bent to form a circular ring on the right. Suppose that the right end of the lattice is coupled to the lattice at the lattice site p. As an illustration, such a lattice with $N = 14$ and $p = 7$ is depicted in Fig. 1(a). As a result, the system satisfies mixed boundary conditions (MBC). In this case, Eq. (1) is modified at $n = p$ (due to the extra coupling at $n = p$),

$$\begin{aligned} &J_R\psi_{n-1} + J_L\psi_{n+1} + V_n\psi_n = E\psi_n \quad (n \neq p), \\ &J_R(\psi_{p-1} + \psi_N) + J_L\psi_{p+1} + V_p\psi_p = E\psi_p, \end{aligned} \tag{2}$$

where p is a site number in the bulk $2 \leqslant p \leqslant N-1$. Note that in order to obtain the solution of the former equation, we use the MBC

$$\psi_0 = 0, \quad \psi_{N+1} = \psi_p. \tag{3}$$

In the Hermitian lattice, $J_L = J_R$, MBC is of no special importance since the extra coupling between the right edge and a bulk point of the lattice has only perturbative effects for a long lattice (the MBC, PBC, and OBC energy spectra almost coincide). On the other hand, in the non-Hermitian lattice, MBC leads to the coexistence of extended (delocalized) and localized eigenstates even in the absence of any on-site potentials. We emphasize that the delocalized states are not extended only in the circular ring, but throughout the whole lattice. Note that such a coexistence was shown to appear in the presence of tailored quasiperiodical potentials and coupling constant [11–24]. However, we see it in our system as a result of the boundary condition sensitivity of the nonreciprocal non-Hermitian systems.

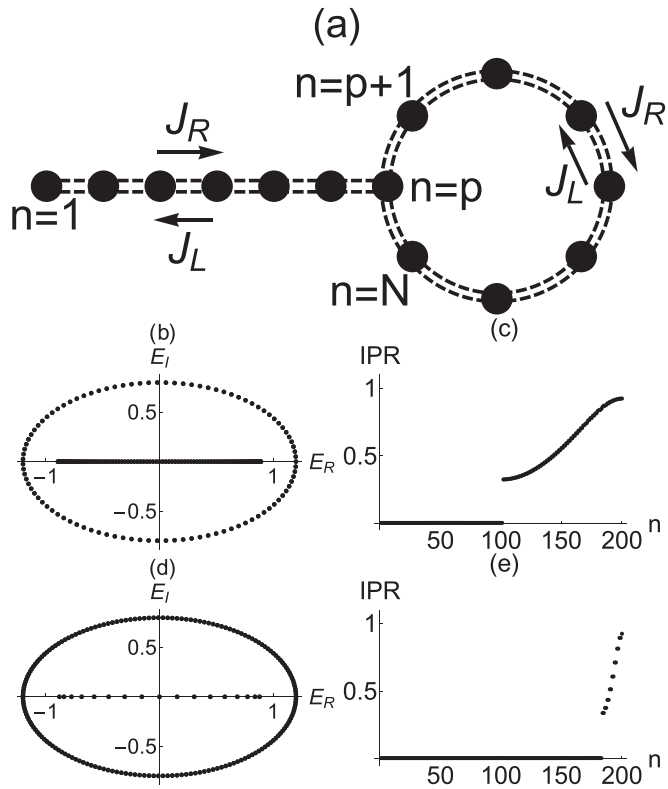

FIG. 1. (a) A representation for a lattice with asymmetrical couplings under MBC with $N = 14$ and $p = 7$. The lattice has one edge and one circular ring. In the ring, the couplings are J_R in the clockwise direction and J_L in the counterclockwise direction. (b) and (d) The energy spectra in the complex plane, where extended states are placed on the loop and localized states are placed on the real axis inside the loop. (c) and (e) The sudden jump from almost zero to a large IPR value indicates the coexistence of extended and localized eigenstates. The numerical parameters are $J_L = 1$, $J_R = 0.2$, $N = 200$, and $p = 100$ [(b) and (c)] and $p = 18$ [(d) and (e)]. The PBC (OBC) spectrum is denser for a (smaller) larger p. The total number of the states with almost zero IPR values are equal to $N - p$.

Let us start with the case without on-site potentials, $V_n = 0$ in a long but finite lattice. The MBC spectrum in the complex plane describes both a line segment on the real axis and a loop that is slightly deformed from the corresponding PBC loop. The states distributed on the MBC loop are extended states, whereas the ones on the line segment are skin states that are exponentially localized at the left edge. The parameter p has the key role on the total number of extended states. In fact, there are $N - p + 1$ extended eigenstates and the rest are all skin states. As a special case, we have only one skin state that is also topologically robust against the coupling disorder at $p = 2$. Oppositely, at $p = N - 1$, there exists one pair of extended states $\{\psi_n, e^{i\pi n}\psi_n\}$ with real energies and all other states are localized skin states. To quantify localization and extension of an eigenstate with eigenvalue E, we can use the inverse participation ratio (IPR)

$$\mathrm{IPR}(E) = \frac{\sum_n |\psi_n(E)|^4}{[\sum_n |\psi_n(E)|^2]^2}. \tag{4}$$

Specifically, IPR is of the order of $1/N$ for an extended eigenstate while it is close to 1 for a localized eigenstate. To illustrate our discussion, we first plot the spectra in the complex plane for two different values of p at $J_L = 1$, $J_R = 0.2$, and $N = 200$ in Figs. 1(b) and 1(d). The points on the loop are very dense for small values of p and become sparse with increasing p at fixed N. The points on the real axis are inside the MBC energy loop. We then plot the IPR values corresponding to the cases Figs. 1(b) and 1(d) in Figs. 1(c) and 1(e). One can notice the gap in these plots where the IPR values jump from almost zero values to nearly 0.4 at $n = p - 1$. This sharp increase of IPR implies the coexistence of localized and extended states in the absence of the disorder. To this end, let us write the analytical solution available for the unidirectional lattice with $J_R = 0$ under MBC. In this case, the extended states are given by $\psi_n = e^{ikn}$ with eigenvalues $E = J_L\, e^{ik}$, where $k = 2\pi\, j(N - p + 1)^{-1}$ and $j = 0, 1, \ldots, N - p$, respectively. On the other hand, the system has an exceptional point and the coalesced skin state is given by $\psi_n = \delta_{n,1}$ with zero energy. Therefore, the corresponding IPR values are $1/N$ for the extended states and 1 for the skin state.

Introducing disorder through random on-site potentials deforms the energy loop in the complex plane at fixed p (contraction in the imaginary axis and elongation in the real axis as the disorder strength increases). Furthermore, it reduces the total number of extended states described by the points on the energy loop and hence increases the total number of localized states described by the points located on the real axis. At weak disorder strength, localized states are mostly skin states localized at the left edge. Beyond the Anderson transition point at which all eigenstates are localized, localization occurs all over the lattice. We plot the IPR values and complex energy spectra in Figs. 2(a) and 2(b) for the system described in Fig. 1 but with various disorder strengths. As can be seen, increasing the disorder strength reduces the total number of extended states until the disorder strength is equal to a critical strength ($W_c \approx 5$) at which Anderson transition occurs. Therefore, there are still some extended eigenstates at $W = 1$ (in black) and $W = 3$ (in blue), but all eigenstates are localized at $W = 8$ (in red). The corresponding spectrum becomes real valued and the OBC and MBC spectra are almost the same when all eigenstates are localized [Fig. 2(b)]. The Anderson transition point also corresponds to a topological phase transition point as we will see below. As a result, we say that extended and localized states coexist only in the topologically nontrivial region. The critical disorder strength at which Anderson transition occurs depends on p at fixed N. Roughly speaking, W_c at fixed N increases slightly with p unless p is close to N at which W_c decreases sharply.

We perform other computations for the quasiperiodical potential $V_n = V_0 \cos(2\pi\beta n)$ and plot the IPR values and energy spectra in Figs. 2(c) and 2(d) and for three different values of V_0 at $\beta = \frac{\sqrt{5}-1}{2}$ and $p = \frac{N}{2}$. At $V_0 = 1$, we see a sharp increase in the IPR values from 0 to nearly 0.3, indicating that almost half of the states are extended while the rest are localized (in black). It is well known that the critical point at which localization-delocalization transition occurs is at 2 in the Hermitian Aubry-Andre model. This value is almost equal

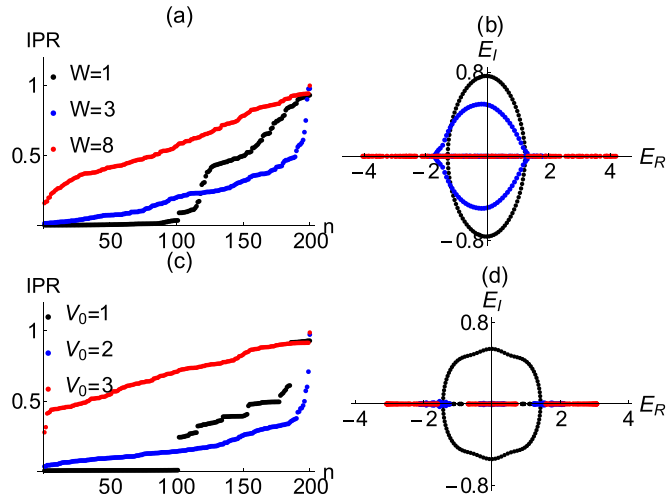

FIG. 2. IPR values and their corresponding energy eigenvalues in the complex plane at various potential strengths for Anderson (a) and (b) and Aubry-André models (c) and (d), respectively, when $J_L = 1$, $J_R = 0.2$, and $N = 2p = 200$. At strong on-site potentials (in red), all eigenvalues lie on the real axis, indicating that all eigenstates are localized. Contrarily, at weak on-site potentials (in black), almost half of the eigenstates are extended while the other half are localized. In the intermediate case (blue), there are still a few extended eigenstates. Note that $V_0 = 2$ is the phase transition point for the quasiperiodical potential. One can see a few extended states with small complex eigenvalues due to the finite number of the lattice sites (localization length is large and it practically becomes extended). (If the lattice is much longer, then one would see its localization character.)

to the critical point for the MBC (a slight perturbation comes from the left edge and coupling between the right edge and the lattice point p). The critical point also coincides with the topological phase transition point as we will see below. One can see a few complex eigenvalues (in blue) at $V_0 = 2$ with complex eigenvalues in Fig. 2(d) (in blue). Beyond the critical point the spectrum is real and all eigenstates are localized ($V_0 = 3$ in red). As a result, we say that extended and localized states coexist in the quasiperiodical lattice under the MBC as long as V_0 is below than the critical number at which a topological phase transition occurs. To this end, in Fig. 3 we plot the curve described by $\{E_R(\beta), E_I(\beta), \beta\}$ for our system under the MBC. Interestingly enough we observe that a three-dimensional butterfly spectra is emerging.

Let us discuss topological features in our system. The spectral winding number ω at the zero base energy for the Hatano-Nelson model in the absence of on-site potentials is equal to 1 when $J_L > J_R$ [50]. The system remains to be in the topological phase in the presence of on-site disorder until the disorder strength is strong enough to make all eigenstates to have real eigenvalues at which the Anderson transition occurs. To compute the topological number in the presence of the on-site potentials under MBC, we follow a similar method introduced in Ref. [50]. Suppose that the coupling constant at the lattice closing point (between Nth and pth sites) are multiplied by $e^{\mp i\Phi}$, where Φ is a fictitious magnetic flux. Then the winding number at zero base energy for a disordered

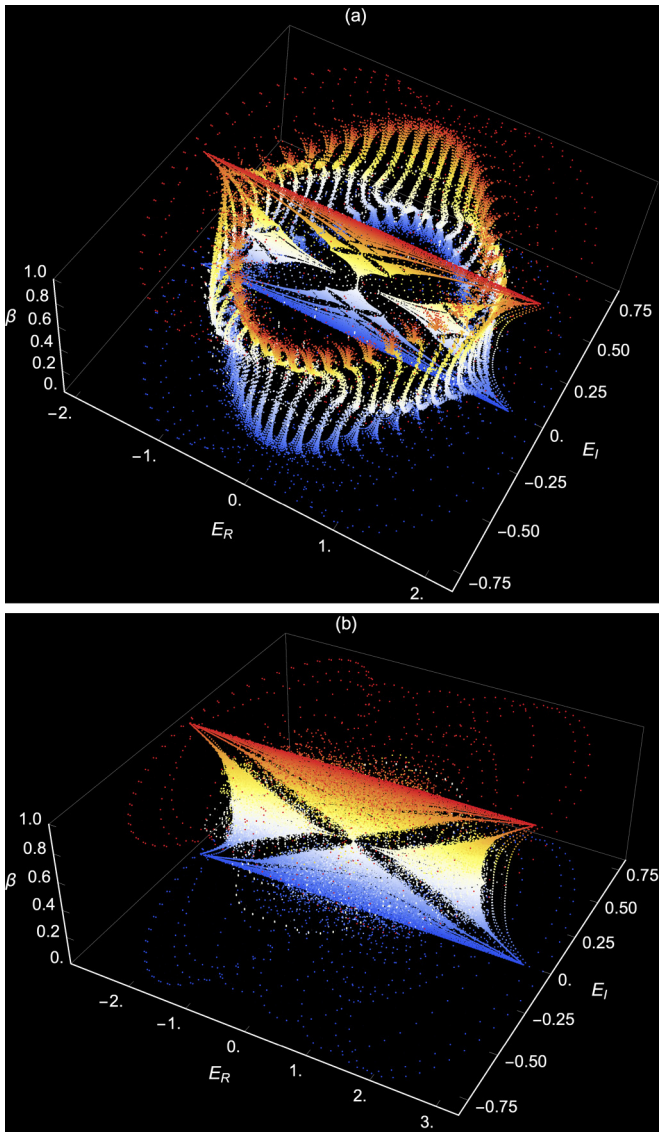

FIG. 3. The butterfly spectra under MBC in three dimensions at $V_0 = 1$ (a) and $V_0 = 2$ (b), where E_R and E_I are real and imaginary parts of the energy eigenvalues. In the two-dimensional complex energy plane with fixed β, the spectrum determines a loop and a line inside the loop as in Fig. 1(b). In three dimensions, where β is the vertical axis, the butterfly shape appears. The parameters are given by $J_L = 1$ and $J_R = 0.2$ and $N = 2p = 100$.

lattice is given by

$$\omega = \int_0^{2\pi} \frac{d\Phi}{2\pi i} \partial_\Phi \ln \det[H(\Phi)], \tag{5}$$

where H is the corresponding Hamiltonian for the model (1) under MBC. The spectral winding number counts the number of times the complex spectral trajectory encircles $E_B = 0$ base energy when Φ varies from zero to 2π. Apparently, the winding number becomes zero when the spectrum is real and all eigenstates are localized. Note that the above formula works well when the number p is not close to N since the spectral loop in the complex plane is less dense when p increases. The MBC lattice is required to be a finite lattice, so we approximate the derivative with a finite difference in the numerical

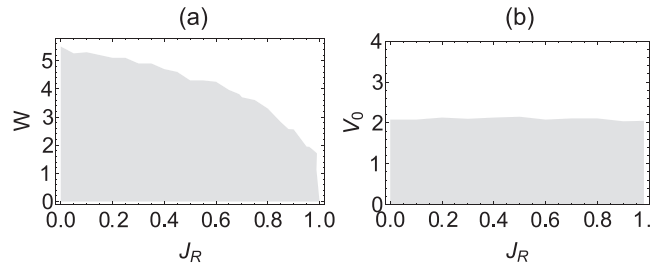

FIG. 4. The critical strengths for the Anderson (a) and Aubry-Andre (b) models under MBC as a function of J_R at $J_L = 1$ and $N = 2p = 200$. The shaded area has winding number $\omega = 1$ and complex spectra. The top unshaded area has zero winding number and real spectra. In the topologically nontrivial region (shaded area), localized and extended states coexist. On the other hand, in the topologically trivial region, only localized states exist.

differentiation. We present our numerical results and plot the winding number as a function of J_R in Fig. 4, where the shaded and unshaded area has $w = 1$ and $w = 0$, respectively. In Fig. 4(a), the critical strength is around $W \approx 5$ at $J_R = 0$ and reduced to zero at $J_R = 1$ (the spectrum becomes real in the Hermitian limit). On the other hand, it is almost constant for the quasiperiodical lattice in Fig. 4(b). Small fluctuations around $V_0 = 2$ is the result of the perturbative effect due to the imposition of the MBC on the finite lattice.

We finally make a brief discussion for $J_R > J_L$. Without loss of generality, we suppose that $J_R = 1$. Consider first that $V_n = 0$. Due to NHSE, bulk states are localized at the right edge under OBC. If we consider the MBC, the right edge is coupled to a bulk point. In this case, there are $N - p + 1$ extended states and the rest are exponentially localized states centered at the bulk point p where the right edge is closed. As opposed to the cases considered above, the extended states are extended only in the circular lattice at any value of J_R and localized states have complex eigenvalues. Therefore, there are multiple energy loops in the complex plane, one for the extended states and another one(s) for the localized states. The localization length of the localized state increases and diffuses more into the straight lattice ($n \leqslant p$) as J_L is increased. In the presence of the disorder, the number of extended states decreases and localized states appear centered at various points of the lattice. If the disorder is sufficiently strong, then Anderson transition takes place and all eigenstates have real eigenvalues and get localized.

III. CONCLUSION

It is generally believed that mobility edges separating extended and localized states in one-dimensional tight-binding models appear if correlated disorder and coupling constants are specially tailored. Here we introduce the mixed boundary conditions to study a finite lattice with one open edge as an alternative to the semi-infinite boundary conditions, which also requires one open edge. The finite lattice we consider is the one whose one edge is bent to form a circular ring and coupled to the lattice at the lattice point p. We have shown that extended and localized states can coexist even without on-site potentials in such a lattice as a result of the boundary

condition sensitivity of the nonreciprocal non-Hermitian systems as long as the system is topologically nontrivial. We have also shown that the total number of extended states is exactly equal to $N - p + 1$, where N is the total number of the lattice sites. In the presence of the disordered on-site potentials, the total number of the extended states reduces with increasing disorder strength and the extended states disappear when the disorder strength is at the critical point at which topological phase transition occurs since the corresponding spectrum become real valued. Experimental observation of mobility edges in non-Hermitian systems often requires complicated designs of couplings or on-site potentials. The mixed boundary conditions can be utilized in non-Hermitian systems to obtain mobility edges more easily.

ACKNOWLEDGMENTS

C.Y. wishes to acknowledge the support from the Scientific and Technological Research Council of Turkey through the 2219 program with Grant No. 1059B191900044. H.R. acknowledges the support by the Army Research Office Grant No. W911NF-20-1-0276 and NSF Grant No. PHY-2012172. The views and conclusions contained in this document are those of the authors and should not be interpreted as representing the official policies, either expressed or implied, of the Army Research Office or the U.S. Government. The U.S. Government is authorized to reproduce and distribute reprints for Government purposes notwithstanding any copyright notation herein.

[1] P. W. Anderson, Absence of diffusion in certain random lattices, Phys. Rev. **109**, 1492 (1958).

[2] S. Aubry and G. André, Analyticity breaking and Anderson localization in incommensurate lattices, Ann. Israel. Phys. Soc. **3**, 133 (1980).

[3] J. Biddle and S. D. Sarma, Predicted Mobility Edges in One-Dimensional Incommensurate Optical Lattices: An Exactly Solvable Model of Anderson Localization, Phys. Rev. Lett. **104**, 070601 (2010).

[4] X. Li, X. Li, and S. Das Sarma, Mobility edges in one-dimensional bichromatic incommensurate potentials, Phys. Rev. B **96**, 085119 (2017).

[5] H. Yao, H. Khouldi, L. Bresque, and L. Sanchez-Palencia, Critical Behavior and Fractality in Shallow One-Dimensional Quasiperiodic Potentials, Phys. Rev. Lett. **123**, 070405 (2019).

[6] T. Liu, X. Xia, S. Longhi, and L. Sanchez-Palencia, Anomalous mobility edges in one-dimensional quasiperiodic models, Sci. Post Phys. **12**, 027 (2022).

[7] G. Roosz, U. Divakaran, H. Rieger, and F. Igloi, Nonequilibrium quantum relaxation across a localization-delocalization transition, Phys. Rev. B **90**, 184202 (2014).

[8] F. Delyon, H. Kunz, and B. Souillard, One-dimensional wave equations in disordered media., J. Phys. A: Math. Gen. **16**, 25 (1983).

[9] H. P. Lüschen, S. Scherg, T. Kohlert, M. Schreiber, P. Bordia, X. Li, S. Das Sarma, and I. Bloch, Single-Particle Mobility Edge in a One-Dimensional Quasiperiodic Optical Lattice, Phys. Rev. Lett. **120**, 160404 (2018).

[10] X. Xia, K. Huang, S. Wang, and X. Li, Exact mobility edges in the non-Hermitian t_1-t_2 model: Theory and possible experimental realizations, Phys. Rev. B **105**, 014207 (2022).

[11] T. Liu, H. Guo, Y. Pu, and S. Longhi, Generalized Aubry-André self-duality and mobility edges in non-Hermitian quasiperiodic lattices, Phys. Rev. B **102**, 024205 (2020).

[12] L. Zhou and W. Han, Non-Hermitian quasicrystal in dimerized lattices, Chin. Phys. B **30**, 100308 (2021).

[13] Y. Wang, X. Xia, Y. Wang, Z. Zheng, and X.-J. Liu, Duality between two generalized Aubry-André models with exact mobility edges, Phys. Rev. B **103**, 174205 (2021).

[14] L. Zhou and Y. Gu, Topological delocalization transitions and mobility edges in the nonreciprocal Maryland model, J. Phys.: Condens. Matter **34**, 115402 (2022).

[15] L.-J. Zhai, G.-Y. Huang, and S. Yin, Cascade of the delocalization transition in a non-Hermitian interpolating Aubry-André-Fibonacci chain, Phys. Rev. B **104**, 014202 (2021).

[16] T. Liu and X. Xia, Real-complex transition driven by quasiperiodicity: A class of non-PT symmetric models, Phys. Rev. B **105**, 054201 (2022).

[17] T. Liu and S. Cheng, Mobility edges in PT-symmetric cross-stitch flat band lattices, arXiv:2105.14724.

[18] L.-M. Chen, Y. Zhou, S. A. Chen, and P. Ye, Quantum entanglement of non-Hermitian quasicrystals, Phys. Rev. B **105**, L121115 (2022).

[19] Y. Liu, X.-P. Jiang, J. Cao, and S. Chen, Non-Hermitian mobility edges in one-dimensional quasicrystals with parity-time symmetry, Phys. Rev. B **101**, 174205 (2020).

[20] Y. Liu, Y. Wang, X.-J. Liu, Q. Zhou, and S. Chen, Exact mobility edges, PT-symmetry breaking, and skin effect in one-dimensional non-Hermitian quasicrystals, Phys. Rev. B **103**, 014203 (2021).

[21] Y. Liu, Y. Wang, Z. Zheng, and S. Chen, Exact non-Hermitian mobility edges in one-dimensional quasicrystal lattice with exponentially decaying hopping and its dual lattice, Phys. Rev. B **103**, 134208 (2021).

[22] L. Li, C. H. Lee, and J. Gong, Impurity induced scale-free localization, Commun. Phys. **4**, 42 (2021).

[23] S. Roy, S. K. Maiti, L. M. Perez, J. H. O. Silva, and D. Laroze, Localization properties of a quasiperiodic ladder under physical gain and loss: Tuning of critical points, mixed-phase zone and mobility edge, Materials **15**, 597 (2022).

[24] C. Wu, J. Fan, G. Chen, and S. Jia, Non-Hermiticity-induced reentrant localization in a quasiperiodic lattice, New J. Phys. **23**, 123048 (2021).

[25] Z.-H. Wang, F. Xu, L. Li, D.-H. Xu, and B. Wang, Topological superconductors and exact mobility edges in non-Hermitian quasicrystals, Phys. Rev. B **105**, 024514 (2022).

[26] X. Zhao, Y. Xing, L. Qi, S. Liu, S. Zhang, and H.-F. Wang, Real-potential-driven anti-PT-symmetry breaking in non-Hermitian Su-Schrieffer-Heeger model, New J. Phys. **23**, 073043 (2021).

[27] S. Mu, L. Zhou, L. Li, and J. Gong, Non-Hermitian pseudo mobility edge in a coupled chain system, Phys. Rev. B **105**, 205402 (2022).

[28] S. Cheng and X. Gao, Majorana zero modes, unconventional real-complex transition, and mobility edges in a

one-dimensional non-Hermitian quasi-periodic lattice, Chin. Phys. B. **31**, 017401 (2022).
[29] L. Li, Ching H. Lee, S. Mu, and J. Gong, Critical non-Hermitian skin effect, Nat. Commun. **11**, 5491 (2020).
[30] L. Pezze and L. Sanchez-Palencia, Localized and Extended States in a Disordered Trap, Phys. Rev. Lett. **106**, 040601 (2011).
[31] T. Chanda, R. Yao, and J. Zakrzewski, Coexistence of localized and extended phases: Many-body localization in a harmonic trap, Phys. Rev. Research **2**, 032039(R) (2020).
[32] Y.-X. Xiao, Z.-Q. Zhang, and C. T. Chan, A band of bound states in the continuum induced by disorder, Sci. Rep. **8**, 5160 (2018).
[33] A. Rodriguez, A. Chakrabarti, and R. A. Römer, Controlled engineering of extended states in disordered systems, Phys. Rev. B **86**, 085119 (2012).
[34] H. Jiang, L.-J. Lang, C. Yang, S.-L. Zhu, and S. Chen, Interplay of non-Hermitian skin effects and Anderson localization in nonreciprocal quasiperiodic lattices, Phys. Rev. B **100**, 054301 (2019).
[35] S. Longhi, Spectral deformations in non-Hermitian lattices with disorder and skin effect: A solvable model, Phys. Rev. B **103**, 144202 (2021).
[36] Y. Liu, Q. Zhou, and S. Chen, Localization transition, spectrum structure, and winding numbers for one-dimensional non-Hermitian quasicrystals, Phys. Rev. B **104**, 024201 (2021).
[37] C. Yuce, PT symmetric Aubry-André model, Phys. Lett. A **378**, 2024 (2014).
[38] J. Claes and T. L. Hughes, Skin effect and winding number in disordered non-Hermitian systems, Phys. Rev. B **103**, L140201 (2021).
[39] L.-Z. Tang, G.-Q. Zhang, L.-F. Zhang, and D.-W. Zhang, Localization and topological transitions in non-Hermitian quasiperiodic lattices, Phys. Rev. A **103**, 033325 (2021).
[40] Q.-B. Zeng and Y. Xu, Winding numbers and generalized mobility edges in non-Hermitian systems, Phys. Rev. Research **2**, 033052 (2020).
[41] C. Yuce, Nonlinear non-Hermitian skin effect, Phys. Lett. A **408**, 127484 (2021).
[42] Y. Yi and Z. Yang, Non-Hermitian Skin Modes Induced by On-Site Dissipations and Chiral Tunneling Effect, Phys. Rev. Lett. **125**, 186802 (2020).
[43] S. Longhi, Topological Phase Transition in non-Hermitian Quasicrystals, Phys. Rev. Lett. **122**, 237601 (2019).
[44] S. Schiffer, X.-J. Liu, H. Hu, and J. Wang, Anderson localization transition in a robust PT-symmetric phase of a generalized Aubry-André model, Phys. Rev. A **103**, L011302 (2021).
[45] Z. Ozcakmakli Turker and C. Yuce, Open and closed boundaries in non-Hermitian topological systems, Phys. Rev. A **99**, 022127 (2019).
[46] C. Yuce, Non-Hermitian anomalous skin effect, Phys. Lett. A **384**, 126094 (2020).
[47] X. Cai, Boundary-dependent self-dualities, winding numbers, and asymmetrical localization in non-Hermitian aperiodic one-dimensional models, Phys. Rev. B **103**, 014201 (2021).
[48] T. Li, Y.-S. Zhang, and W. Yi, Engineering dissipative quasicrystals, Phys. Rev. B **105**, 125111 (2022).
[49] N. Hatano and D. R. Nelson, Localization Transitions in Non-Hermitian Quantum Mechanics, Phys. Rev. Lett. **77**, 570 (1996).
[50] Z. Gong, Y. Ashida, K. Kawabata, K. Takasan, S. Higashikawa, and M. Ueda, Topological Phases of Non-Hermitian Systems, Phys. Rev. X **8**, 031079 (2018).